Hydrol. Earth Syst. Sci., 28, 1527–1538, 2024
https://doi.org/10.5194/hess-28-1527-2024

Hydrology and Earth System Sciences
Open Access
EGU

Sediment transport in South Asian rivers high enough to impact satellite gravimetry

Alexandra Klemme[1], Thorsten Warneke[1], Heinrich Bovensmann[1], Matthias Weigelt[2], Jürgen Müller[2], Tim Rixen[3], Justus Notholt[1], and Claus Lämmerzahl[4]

[1]Institute of Environmental Physics, University of Bremen, Otto-Hahn-Allee 1, 28359 Bremen, Germany
[2]Institute of Geodesy, Leibniz Universität Hannover, Schneiderberg 50, 30167 Hannover, Germany
[3]Leibniz Centre for Tropical Marine Research, Fahrenheitstr. 6, 28359 Bremen, Germany
[4]Centre of Applied Space Technology and Microgravity, University of Bremen, Am Fallturm 2, 28359 Bremen, Germany

Correspondence: Alexandra Klemme (aklemme@uni-bremen.de)

Received: 31 January 2023 – Discussion started: 3 March 2023
Revised: 10 November 2023 – Accepted: 23 January 2024 – Published: 4 April 2024

Abstract. Satellite gravimetry is used to study the global hydrological cycle. It is a key component in the investigation of groundwater depletion on the Indian subcontinent. Terrestrial mass loss caused by river sediment transport is assumed to be below the detection limit in current gravimetric satellites of the Gravity Recovery and Climate Experiment Follow-On mission. Thus, it is not considered in the calculation of terrestrial water storage (TWS) from such satellite data. However, the Ganges and Brahmaputra rivers, which drain the Indian subcontinent, constitute one of the world's most sediment-rich river systems. In this study, we estimate the impact of sediment mass loss within their catchments on local trends in gravity and consequential estimates of TWS trends. We find that for the Ganges–Brahmaputra–Meghna catchment sediment transport accounts for (4 ± 2) % of the gravity decrease currently attributed to groundwater depletion. The sediment is mainly eroded from the Himalayas, where correction for sediment mass loss reduces the decrease in TWS by 0.22 cm of equivalent water height per year (14 %). However, sediment mass loss in the Brahmaputra catchment is more than twice that in the Ganges catchment, and sediment is mainly eroded from mountain regions. Thus, the impact on gravimetric TWS trends within the Indo–Gangetic Plain – the main region identified for groundwater depletion – is found to be comparatively small (< 2 %).

1 Introduction

Since March 2002, the Gravity Recovery and Climate Experiment (GRACE) mission provides satellite-based measurements of the Earth's gravity field (Dahle et al., 2019), with the only major data gap being between the end of the original satellite mission in August 2017 and the launch of the follow-on mission (GRACE-FO) in May 2018. Gravity fields derived from satellite measurements yield information on global mass variations, which have proven crucial to monitor changes in global water storage and fluxes (Rodell et al., 2018). Retrieved data of the mass equivalent water height (EWH) are widely used for studies on topics such as glacier melting (Jacob et al., 2012; Luthcke et al., 2013), groundwater depletion (Rodell et al., 2009; Xie et al., 2020) and sea level rise (Cazenave et al., 2009; Jeon et al., 2018).

One significant region that yields negative trends in terrestrial water storage (TWS) is north-west India with an average decrease of $(29 \pm 2.5)\,\mathrm{m^3\,H_2O\,yr^{-1}}$ (Rodell et al., 2018; Xie et al., 2020). Several studies have investigated this decrease and explained it by a large-scale groundwater loss due to excessive extraction for irrigation (Tiwari et al., 2009; Rodell et al., 2009; Panda and Wahr, 2016; Rodell et al., 2018; Xie et al., 2020). Wada et al. (2012) found that the use of non-renewable groundwater for irrigation more than tripled since 1960. In the year 2000, one-fifth of the global irrigation water demand was fed by non-renewable groundwater abstraction, with the majority being abstracted in India and Pakistan (Wada et al., 2012). Furthermore, the depletion in In-

dian groundwater occurred during a period of increased precipitation, implying an even stronger water deficit for future droughts (Rodell et al., 2018).

A large fraction of the Indian subcontinent is drained by the Ganges–Brahmaputra river system. The Ganges and Brahmaputra rivers originate in the Himalayan belt and drain intensely cultivated regions before their confluence in Bangladesh and discharge into the Bay of Bengal (Subramanian and Ramanathan, 1996; Garzanti et al., 2011). These rivers are one of the largest sources of water and sediment for the world's ocean (Akter et al., 2021). The high amounts of sediment they carry into the Bay of Bengal make up the Bengal Delta and submarine fan that extends from Bangladesh to south of the Equator and contains at least 1.1×10^{19} kg of sediment with an average accumulation rate of 665×10^9 kg yr^{-1} (Curray, 1994). The sediment transport by the Ganges–Brahmaputra river system shows strong diurnal, seasonal and inter-annual variations (Subramanian and Ramanathan, 1996). Estimates of sediment discharge vary widely between 200×10^9 and 1600×10^9 kg yr^{-1} for the Ganges river (Rahman et al., 2018; Holeman, 1968) and between 150×10^9 and 1157×10^9 kg yr^{-1} for the Brahmaputra river (Akter et al., 2021; Milliman and Meade, 1983). Yet, recent studies state the annual combined sediment discharge of the rivers to be about 10^{12} kg with the majority being carried during the monsoon season from June to October (Wasson, 2003; Kuehl et al., 2005; Wilson and Goodbred, 2015; Mouyen et al., 2018; Mahmud et al., 2020; Akter et al., 2021).

This river sediment transport implies a terrestrial mass reduction that has so far not been considered in the computation of gravimetric TWS data. A study by Schnitzer et al. (2013) found that the mass loss associated with the large-scale soil erosion in the Chinese Loess Plateau was not visible considering the available GRACE resolution. However, recent studies found the sediment discharge to the ocean to be visible using satellite gravimetry of the estuary regions (Mouyen et al., 2018; Li et al., 2022). While the incorporation of sediment mass loss into monthly GRACE solutions over land might be impossible at the current satellite resolutions, it is a non-negligible loss when considering long-term TWS trends studied in regard to, for example, groundwater depletion.

Additional processes to consider in long-term gravimetric data are plate tectonics. The Himalayan mountain range experiences uplift due to the tectonic collision between the Indian and the Eurasian continental plates. The gravimetric impact of this process is not the focus of this study. Yet, knowledge of such additional tectonic processes is essential to contextualize the resulting sediment impact, as the increase in mass due to this Himalayan mountain uplift could counteract part of the mass loss due to sediment erosion and discharge.

In this study, we estimate the impact of mass loss due to soil erosion and sediment transport by major rivers draining the Indian subcontinent on TWS trends observed by the GRACE and GRACE-FO satellites.

2 Methods

2.1 Study Area

This study focuses on the Ganges and Brahmaputra catchments, with some discussion of the Indus and Meghna catchments. The rivers are located mainly in northern India but also partly flow through China, Pakistan, Nepal, Bhutan, Afghanistan and Bangladesh (Fig. 1). The river catchments are impacted by the South Asian monsoon, bringing high precipitation and river discharge from June to October. The Ganges and Brahmaputra rivers originate in the Himalayan mountain belt and discharge into the Bay of Bengal after confluence with the Meghna river in Bangladesh. Together with the Indus river, they drain the majority of the Himalayas.

Due to high erosion rates in the Himalayan mountain region, sediment concentrations in these rivers are among the highest worldwide (Subramanian and Ramanathan, 1996; Akter et al., 2021). Especially the Brahmaputra catchment has a large mountain fraction, while the other river catchments show higher agricultural fractions (Table 1). A map including the locations of mountain ranges and agricultural land as well as more detailed river descriptions is included in the Supplement.

India hosts the world's largest groundwater-reliant agricultural irrigation system (Xie et al., 2020). Of its total irrigation-equipped area (620 000 km^2), about 64 % can be irrigated with groundwater, amounting to a total consumptive groundwater use for irrigation of about 200 km^3 yr^{-1} (Siebert et al., 2010). The fraction of irrigation reliant on groundwater has increased over the past decades from only 29 % in 1951 to more than 50 % in 2022 (FAO, 2022), with the absolute groundwater irrigated area being more than 5 times larger than in 1951 (Siebert et al., 2010; FAO, 2022). The major groundwater aquifer for the studied regions is located in the Indo–Gangetic Plain and stretches mainly beneath the Indus and Ganges floodplains, while there are only shallow aquifers in the Himalayan mountain regions (Fig. S2 in the Supplement).

2.2 Gravimetry and sediment data

Gravimetry data in this study are from the GRACE and GRACE-FO satellites. We use post-processed data from the Combination Service for Time-variable Gravity Fields (COST-G) Level-3 data product (Boergens et al., 2020) for TWS anomalies in measures of EWH. The data are based on the COST-G RL01 Level-2B products by Dahle and Murböck (2020) and include gridded data for TWS, TWS uncertainty, spatial leakage contained in the TWS and the background model atmospheric mass, all in a monthly resolution

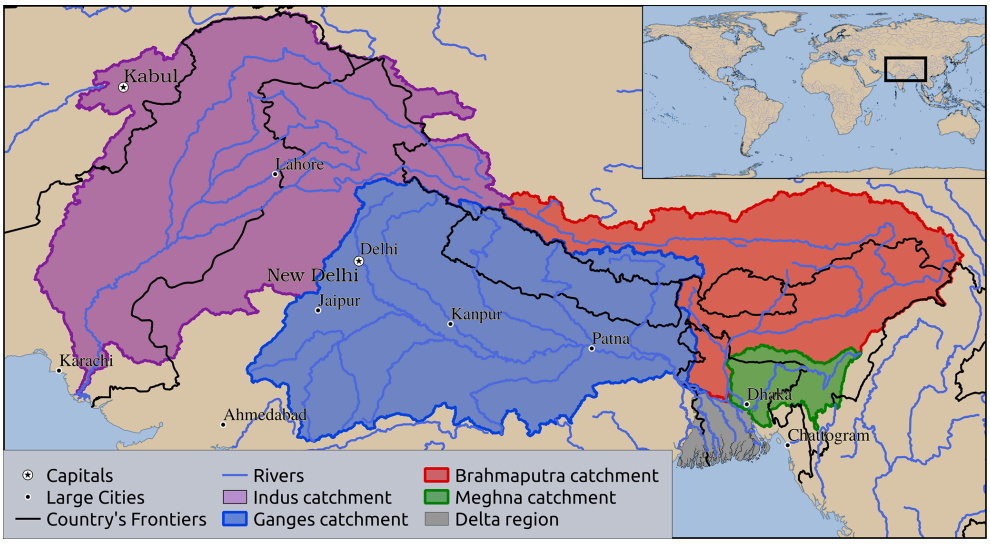

Figure 1. Map of investigated catchments (Lehner and Grill, 2013) and river paths (GRDC, 2020).

Table 1. Mountain and agricultural fractions of the catchments.

	Total	GBM	Ganges	Brahmaputra	Meghna	Indus
Catchment area (km^2)	2 679 069	1 576 134	950 754	539 989	85 391	1 102 935
Mountain fraction (%)	36.0	32.9	15.9	67.4	3.3	51.6
Agricultural fraction (%)	45.6	39.3	65.2	18.2	42.8	34.4

Total refers to the combined Ganges, Brahmaputra, Meghna and Indus catchments. GBM is the Ganges–Brahmaputra–Meghna catchment. Mountain fraction refers to regions of elevation $\geq$ 1500 m based on elevation data from Jarvis et al. (2008). Agricultural regions are from GLCNMO (2017). River catchment data are from Lehner and Grill (2013).

of $1° \times 1°$. The potential impact of filtering and spatial leakage in these data is discussed in the Supplement.

Monthly TWS anomalies within the investigated catchments are derived by selecting all data whose grid centres are located within the respective catchment and calculating their area-weighted average for each month. Data uncertainty is derived analogously from the area-weighted average of the TWS uncertainties provided in the COST-G data product. Linear least-squares optimizations of the generated monthly time series yield the local TWS trends. Trend uncertainties contain the standard error of the derived slope optimization as well as the uncertainty of the monthly time series. A more detailed trend analysis is included in the Supplement.

Sediment data for this study were collected from the literature. Generally, measurements in the study area are scarce, and existing data are located close to Bangladesh, providing no information on the areal distribution of sediment loss in the upper catchments. The Supplement provides a discussion on this scarcity in sediment data and the consequences for our study. Complete lists of the sediment data and their sources for the Ganges and Brahmaputra rivers are available in Tables S1 and S2 in the Supplement, respectively.

3 Results and discussions

3.1 Geodetic observations of the decrease in terrestrial water storage

Gravimetric data of TWS generally show negative trends within the studied catchments. Trends are most pronounced in the eastern Brahmaputra catchment and in the western Ganges catchment at the border to the Indus catchment. The data yield the strongest decline of 5.8 cm yr^{-1} in north-west India at about 28° N, 76° E (Fig. 2).

Comparisons of average TWS trends within the individual catchments yield the strongest decrease for the Ganges catchment, followed by the Brahmaputra and Indus catchments. The Meghna catchment shows the weakest trend (Table 2). Low standard deviation of trends in the Brahmaputra and Meghna catchments imply rather homogeneous distributions of the TWS decrease in those catchments (Table 2). Higher standard deviations in the Ganges and Indus catchments (Table 2) are likely caused by the distinct negative trend in north-west India. This is confirmed further by the comparatively low median trend values within these catchments (Table 2).

Table 2. Loss of terrestrial water storage within the catchments.

TWS loss ($cm\,yr^{-1}$)	Total	GBM	Ganges	Brahmaputra	Meghna	Indus	Ganges-m	Brahmaputra-m
Mean	1.35	1.51	1.63	1.45	0.60	1.13	1.56	1.60
Median	1.09	1.32	1.24	1.46	0.62	0.57	1.30	1.68
Standard deviation	1.43	1.36	1.67	0.64	0.35	1.49	0.71	0.66
Minimum	−1.12	−1.12	−1.12	0.27	0.09	−0.48	0.94	0.28
Maximum	5.78	5.77	5.77	2.64	1.17	5.78	3.40	2.64

Data show the loss of TWS (in cm) of equivalent water height per year. Negative values represent a water increase. GBM is the combined Ganges–Brahmaputra–Meghna catchment. Total refers to the combination of the Ganges, Brahmaputra, Meghna and Indus catchments. Ganges-m and Brahmaputra-m refer to the mountain regions (altitude ≥ 1500 m) within the Ganges and Brahmaputra catchments, respectively. Data were derived based on pixel-wise linear least-squares fits of the COST-G GRACE data. The mean values are weighted by the different pixel areas, while the other statistical variables do not consider respective pixel sizes.

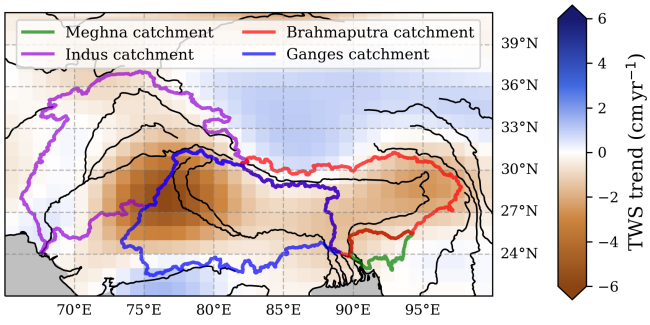

Figure 2. Trend of satellite-based terrestrial water storage (TWS) with location of major river basins on the Indian subcontinent. Data were derived from linear least-squares approximations of the COST-G data (Boergens et al., 2020), based on the GRACE and GRACE-FO time period of April 2002 to December 2022. Locations of river catchments are from Lehner and Grill (2013).

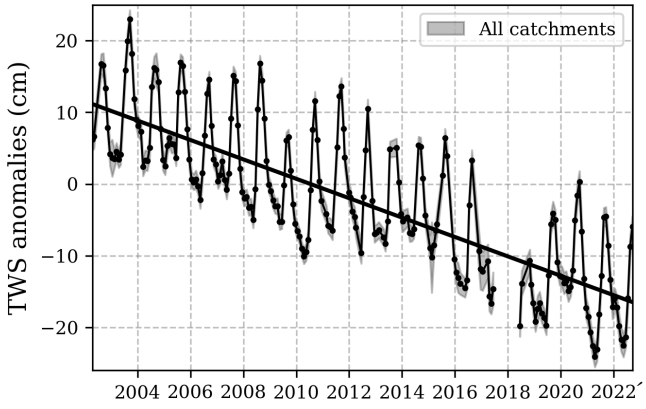

Figure 3. Time series of average terrestrial water storage (TWS) anomalies within the combined Ganges, Brahmaputra, Meghna and Indus catchments. Data points are area-weighted monthly averages within the catchments, and shaded areas represent area-weighted uncertainties stated in the COST-G data product (Boergens et al., 2020). The linear trend was derived based on ordinary least-squares optimization of monthly data. The data gap represents the time between the end of the initial GRACE mission and the start of the GRACE-FO mission.

Additional assessment of TWS trends in catchment mountain regions yields similar results for the Ganges and the Brahmaputra catchments (Table 2). For the Brahmaputra catchment, the observed TWS decrease is slightly higher than for the catchment average. For the Ganges catchment, it is slightly lower than the catchment average (Table 2). While the centre of the main TWS decrease in the Ganges catchment is located in the Indo–Gangetic Plain, it extends into the Ganges mountain ranges. This implies that the TWS decrease in the Ganges mountain regions could be overestimated due to the impact of TWS leakage caused by data filtering, as discussed in the Supplement.

For the combined study area, the average TWS decrease derived from satellite data is $(1.4 \pm 0.2)\,cm\,yr^{-1}$. The time series of TWS in the study area decreases fairly linearly with annual variations, mainly driven by precipitation patterns that cause increasing TWS during the monsoon months and decreasing TWS during dry periods (Fig. 3). This TWS decrease over the complete study area represents a mass reduction of $36 \times 10^{12}\,kg\,yr^{-1}$.

3.2 Mass loss caused by river sediment transport

To estimate the impact of sediment transport on the observed trend in gravity anomalies, we need the total sediment discharge from the studied regions. Based on data collected in various studies, the annual sediment discharge from the Ganges and Brahmaputra rivers is 501×10^9 and $596 \times 10^9\,kg\,yr^{-1}$, respectively (Table 3). Sediment discharge from the Indus river is $168 \times 10^9\,kg\,yr^{-1}$, and the Meghna river discharges $11 \times 10^9\,kg$ of sediment per year (Table 3). The high sediment values in the Ganges and Brahmaputra rivers are caused by their origin in the Himalayan mountains, as those are highly erosion-prone regions. The Meghna river originates in the Indian Naga Hills at less than 2 000 m elevation and mainly drains the floodplains. The Indus river originates in the Himalayas. However,

Table 3. River sediment transport within the catchments.

Sediment load (10^9 kg yr^{-1})	Total	GBM	Ganges	Brahmaputra	Indus	Meghna
Mean	1276	2008	501	596	168	11
Median	1207	1082	480	590	125	12
Standard deviation	633	511	272	237	122	2
Minimum	400	350	200	150	50	0
Maximum	3147	2777	1600	1157	370	20

Sediment loads as compiled from the literature. Total refers to the sum of sediment discharge in all four rivers. GBM refers to sediment discharge in the Ganges–Brahmaputra–Meghna river system. The complete lists of data compiled for the Ganges and Brahmaputra rivers are in Tables S2 and S3, respectively, in the Supplement. Sediment load in the Meghna river is compiled from Coleman (1969), Smith et al. (2009) and Rahman et al. (2018). Sediment load in the Indus river is compiled from Holeman (1968), Milliman and Meade (1983), Giosan et al. (2006) and Mouyen et al. (2018).

its annual sediment discharge has been strongly reduced by the instalment of dams along the river.

Due to data scarcity, it is difficult to assess spatially resolved data for sediment-induced gravity changes in the Indian subcontinent. In the following, we separate between sediment eroded from specific mountain regions based on published literature (Wasson, 2003; Galy et al., 2007; Faisal and Hayakawa, 2022). Additionally, a discussion of spatially resolved sediment loss based on soil loss data from the Revised Universal Soil Loss Equation (RUSLE; Borrelli et al., 2017) is included in the Supplement.

The majority of sediment is discharged during the monsoon season from June to October, when there is also high water discharge in the rivers (Islam, 2016). Over the considered period of GRACE measurements (2002–2022), the rivers discharged more than 25 Pg of sediment. The average discharge rate is roughly 1.3×10^{12} kg yr^{-1} (Table 3).

3.3 Discussion of data seasonality

The seasonality of both TWS anomalies and river sediment discharge depends on the South Asian monsoon. As such, both parameters follow the seasonality of regional precipitation with the sediment discharge peaking approximately 1 month after the precipitation maximum and the TWS peaking 1 month after that (Fig. 4). Since the monsoon moves from the south-east over the Indian subcontinent, precipitation in the Brahmaputra and Meghna catchments starts to increase earlier in the year and more gradually, while precipitation in the Ganges and Indus catchments starts later and increases more rapidly.

This difference in precipitation patterns is also visible in the sediment discharge and TWS anomalies. For the Brahmaputra river, sediment discharge and TWS in the river catchment yield minima in February and show a gradual increase until the monsoon peak in July (Fig. 4). After that, sediment discharge decreases with the precipitation decrease, while TWS stays high until October, when precipitation rates drop below 5 mm d^{-1}. Parameters in the Meghna catchment follow a similar seasonality, whereat precipitation and TWS anomalies are more pronounced in that catchment. Yet, sediment discharge is an order of magnitude weaker than in the Brahmaputra catchment.

For the Ganges river, sediment discharge increases from June to August and decreases from September to November. TWS anomalies in the Ganges catchment increase between June and August and show a steady decline from September to June, when the precipitation rate is below 6 mm d^{-1} (Fig. 4). In the Indus catchment, precipitation rates and TWS anomalies show only small changes during the monsoon season. Additionally, these parameters yield a second local maximum between February and April (Fig. 4). This is likely caused by mid-latitude extra-tropical western disturbances in the southern part of the catchment (Cannon et al., 2015). The Indus sediment discharge shows only the one maximum during monsoon season.

Generally, the mass change due to sediment transport reduces gravity values during TWS increase and does not effect gravity observations during TWS decrease. However, the sediment mass loss in measures of EWH show values that are 3 orders of magnitude smaller than the seasonality observed in GRACE data. This monthly sediment impact is within the uncertainty of monthly gravimetry data and will not considerably impact this study's analysis. While seasonality is included in the following data, we will from here on focus on linear trends in both water and sediment loss.

3.4 Impact of sediment transport on geodetic observations of trends in terrestrial water storage

3.4.1 Impact within the full study area

To compare the mass loss from river sediment transport to the observed TWS trends, the absolute sediment mass loss is divided by the respective catchment area and the density of water. This yields the impact of sediment mass loss in measures of EWH. Considering the total catchment size of the Ganges, Brahmaputra, Meghna and Indus rivers (Table 1) as well as their combined sediment discharge (Table 3), this yields an absolute sediment mass impact of roughly 0.5 mm yr^{-1} that is not considered when deriving TWS based on gravimetric observations. Accordingly, this sediment mass loss needs to

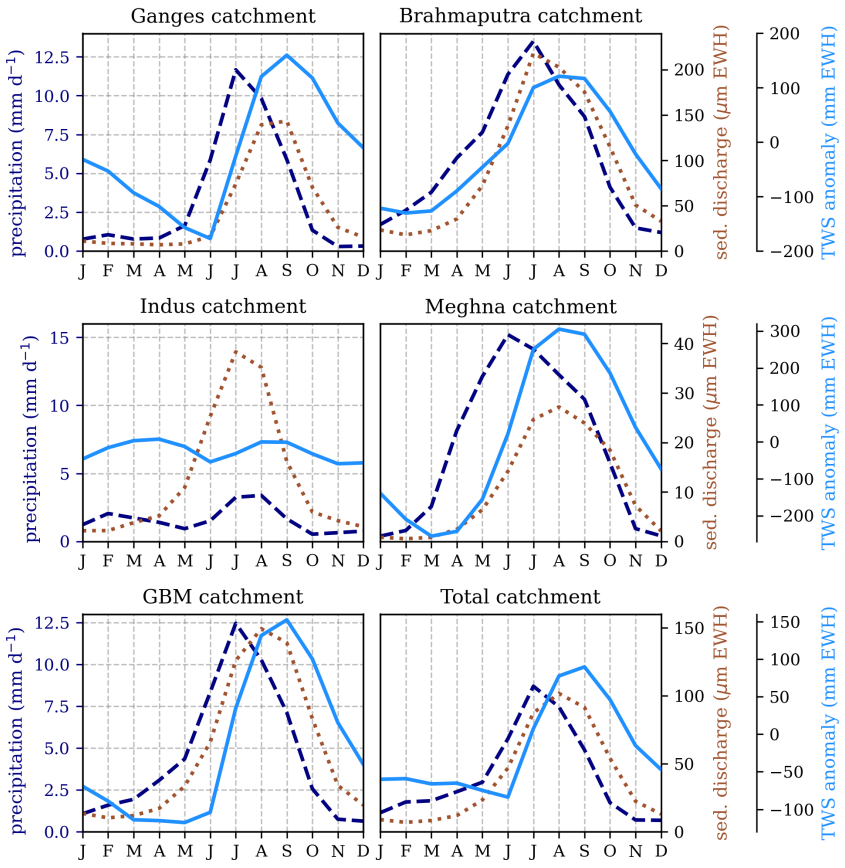

Figure 4. Average seasonality of the precipitation (dashed); the terrestrial water storage (TWS, solid); and the sediment discharge (dotted) within the individual Ganges, Brahmaputra, Indus, and Meghna catchments as well as the combined Ganges–Brahmaputra–Meghna catchment (GBM) and the total combined GBM and Indus catchments (Total). Precipitation data are averaged from the ERA5 reanalysis product for 2000–2022 (Hersbach et al., 2023). Seasonal TWS anomalies are averaged for the COST-G data product for 2002–2022 Boergens et al. (2020). Seasonality of sediment discharge is based on river water discharge according to data in Islam (2016).

be subtracted from the observed trends in TWS anomalies, reducing the local TWS trend of 1.35 cm yr^{-1} by roughly 4 % (Table 4, Fig. 5).

The average monthly sediment impact on TWS observations is less than 0.01 cm of EWH, which is well within the uncertainties stated for GRACE TWS data in the study area (average $\mathrm{TWS_{std}} \approx 1.4$ cm; Boergens et al., 2020). However, considering the whole 20-year time series, our results imply that a gravity decrease corresponding to 1 cm EWH currently attributed to groundwater depletion on the Indian subcontinent could be caused by sediment transport instead.

Exclusion of the Indus catchment yields a stronger relative impact of sediment mass loss on the observed TWS trend for the Ganges–Brahmaputra–Meghna catchment. This is caused by higher sediment discharge per catchment area (Table 4). The measured TWS decrease in the Ganges–Brahmaputra–Meghna catchment is slightly higher than for the complete study area (Fig. 5). The absolute sediment impact on gravity is 0.7 kg m^{-2} yr^{-1}. This represents about 4.6 % of the observed gravity reduction in the Ganges–Brahmaputra–Meghna catchment that is currently attributed to groundwater loss (Table 4). Over the total GRACE data period, correction for this sediment mass loss would reduce the estimated TWS loss by about 1.6 cm.

3.4.2 Impact within individual catchments

Investigation of the individual river catchments yields the highest sediment mass loss for the Brahmaputra catchment (Table 4). This is consistent with the high fraction of mountains in this catchment (Table 1) and high precipitation rates that enhance erosion in the eastern Himalayas (Fig. 4; Burbank et al., 2012). The absolute sediment mass loss in the Ganges catchment is similar to that in the Brahmaputra catchment (Table 4). However, the Ganges catchment is larger than the Brahmaputra catchment, resulting in a sediment impact per catchment area that is only half that in the Brahmaputra catchment (Table 4). Sediment mass loss in the Meghna and Indus catchments is significantly lower than in the Ganges and Brahmaputra catchments (Table 4).

Table 4. Sediment impact on gravimetric observations of TWS trends for studied catchments.

River	Catchment area (km^2)	Sediment loss (10^{12} kg yr^{-1})	GRACE TWS loss (mm yr^{-1})	Abs. sediment impact (kg m^{-2} yr^{-1} ≈ mm yr^{-1})	Rel. sediment impact (%)
Total	2 679 069	1.28 ± 0.63	13.5 ± 2.2	0.48 ± 0.23	3.6 ± 2.3
GBM	1 576,134	1.11 ± 0.51	15.1 ± 2.7	0.70 ± 0.32	4.6 ± 3.0
Ganges	950 754	0.50 ± 0.27	16.3 ± 2.8	0.53 ± 0.29	3.3 ± 2.3
Brahmaputra	539 989	0.60 ± 0.24	14.5 ± 2.6	1.10 ± 0.44	7.6 ± 4.4
Meghna	85 391	0.011 ± 0.002	6.0 ± 4.0	0.13 ± 0.02	2.2 ± 1.8
Indus	1 102 935	0.17 ± 0.12	11.3 ± 1.9	0.15 ± 0.11	1.3 ± 1.2
Ganges-m	148 948	0.50 ± 0.27[b]	15.6 ± 2.5	3.36 ± 1.83	21.5 ± 15.2
Ganges-HH	57 025	0.45 ± 0.27	15.6 ± 2.5[a]	7.89 ± 4.74	50.6 ± 38.6
Ganges-LH	91 885	0.05 ± 0.05	15.6 ± 2.5[a]	0.54 ± 0.54	3.5 ± 4.0
Brahmaputra-m	361 509	0.60 ± 0.24[b]	16.1 ± 2.3	1.65 ± 0.66	10.3 ± 5.6
Brahmaputra-NBS	21 600	0.27 ± 0.20	16.1 ± 2.3[a]	12.50 ± 9.26	77.6 ± 68.6
Brahmaputra-rem.	339 900	0.33 ± 0.22	16.1 ± 2.3[a]	0.97 ± 0.65	6.0 ± 4.9

Total refers to the combined Ganges, Brahmaputra, Meghna and Indus catchments. GBM is the Ganges–Brahmaputra–Meghna catchment. Ganges-m and Brahmaputra-m refer to the mountain regions (altitude ≥ 1500 m) within the Ganges and Brahmaputra catchment, respectively. Ganges-HH and Ganges-LH refer to the High Himalayas and the Lesser Himalayas in the Ganges catchment, respectively. Brahmaputra-NBS and Brahmaputra-rem. refer to the Namcha Barwa syntaxis and the remaining Brahmaputra mountains, respectively. [a] TWS trends within specific locations in the catchment mountain regions are approximated by the average TWS trend over the mountains. [b] Sediment data for the mountain regions assume all river sediment being eroded from these regions.

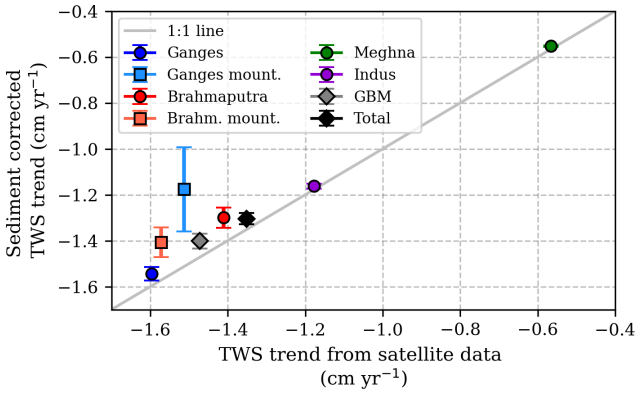

Figure 5. Comparison plot between regional trends in terrestrial water storage (TWS) derived from the COST-G data product (Boergens et al., 2020) and the trends corrected for sediment mass loss. Data points include the individual catchments as well as the combined Ganges–Brahmaputra–Meghna catchment (GBM); the total combined Indus, Ganges, Brahmaputra, and Meghna catchments (Total); and the mountain fractions of the Ganges (Ganges mount.) and Brahmaputra (Brahm. mount.) catchments. Full time series of TWS data with and without sediment correction are included in the Figs. S16 to S21.

The Brahmaputra catchment also yields the highest relative impact of sediment mass loss on the observed gravity trend (Table 4). Correction for this impact reduces the TWS decline by 7.8 %, which over the whole GRACE data period represents more than 2 cm (Fig. 6). In the Ganges catchment, sediment transport represents 3.3 % of the gravity decrease, and the impact within the Indus and Meghna catchments is even smaller (Fig. 5).

3.4.3 Impact within the Himalayan mountain regions

Studies agree that the majority of sediment discharged into the Bay of Bengal is derived from the Himalayan mountain ranges (Wasson, 2003; Galy et al., 2007; Faisal and Hayakawa, 2022). Thus, we specifically studied the impact of sediment mass loss in these regions.

The Brahmaputra catchment includes a mountain fraction of 67.4 % (Table 1). Assuming all of the river's sediment to be derived from these regions yields a sediment mass loss of 1.7 kg m^{-2} yr^{-1} (Table 4). Considering the average TWS decrease derived from GRACE data for the region (Table 4), the sediment mass loss accounts to roughly 10 % of the gravity decrease (Fig. 7). According to Faisal and Hayakawa (2022), about half ((45 ± 15) %) of Brahmaputra's sediment is derived from the Namcha Barwa syntaxis, the easternmost Himalayan syntaxis that encompasses only ≈ 4 % of the Brahmaputra catchment. The remaining sediment is derived from Himalayan tributaries that join the Brahmaputra in the Himalayan foreland (Faisal and Hayakawa, 2022). This indicates that local sediment mass loss within the Namcha Barwa syntaxis and the remaining Brahmaputra mountain areas represent 78 % and 6 % of the observed gravity decrease, respectively (Table 4).

The Ganges catchment includes a mountain fraction of only 15.9 % (Table 1). Even though sediment discharge in the Ganges river is smaller, the area-weighted mass loss over the mountains is about double that of the Brahmaputra mountains (Table 4). Considering the higher TWS decrease in the Ganges mountains, this sediment mass loss accounts for 22 % of the gravity decrease observed in the area (Fig. 7). According to Faisal and Hayakawa (2022), (90 ± 5) % of the

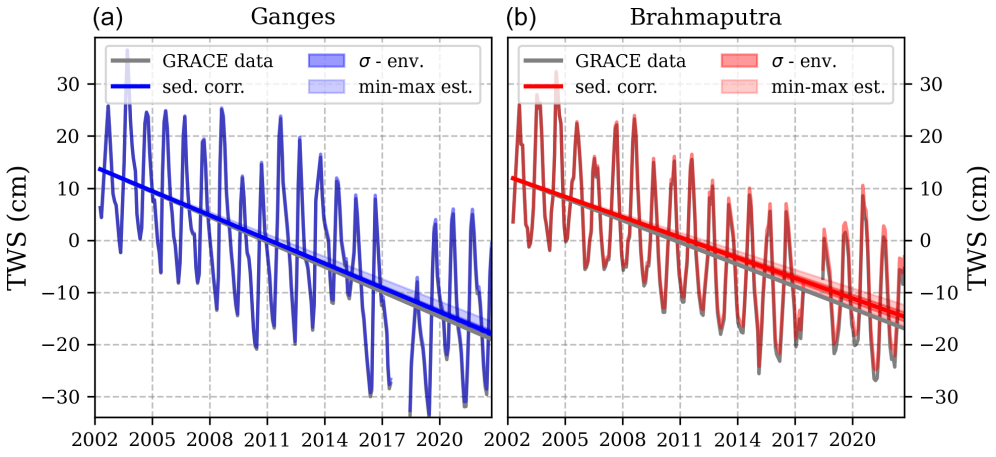

Figure 6. Time series of TWS derived from GRACE data (grey) and TWS data corrected for sediment mass loss (colour). Data show average over the whole Ganges **(a)** and Brahmaputra **(b)** catchments. Ranges for the σ environment (σ - env.) and the min–max estimates refer to the standard deviation and minimum and maximum estimates, respectively, of sediment discharge as stated in Table 3. Analogue figures for all catchments can be found in Figs. S16 to S21.

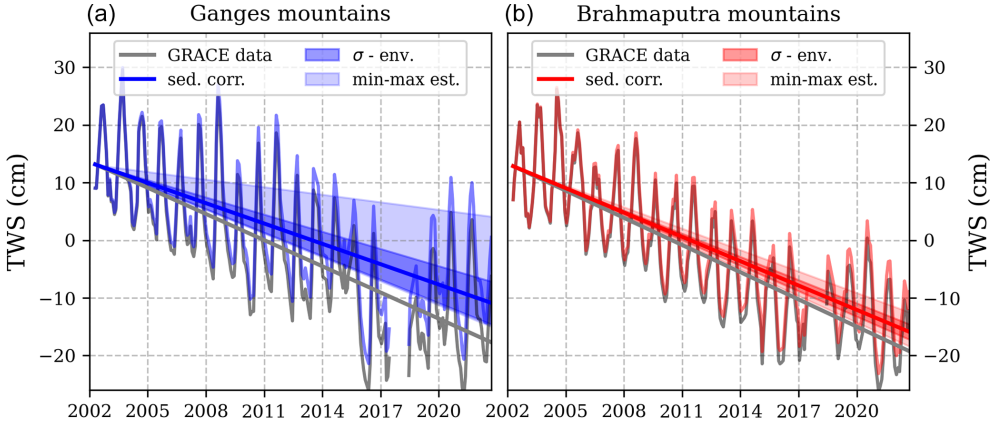

Figure 7. Time series of TWS derived from GRACE data (grey) and TWS after the correction for sediment mass loss (colour). Data show average over the mountain fraction within the Ganges catchment **(a)** and the Brahmaputra catchment **(b)**. σ environment (σ - env.) and min–max estimates refer to the standard deviation and minimum and maximum estimates, respectively, of sediment discharge as stated in Table 3. An analogous figure for the mountain sub-regions is included in Fig. S22.

Ganges sediment is derived from the High Himalayas. The remaining sediment is mostly from the Lesser Himalayas (Wasson, 2003) with a smaller contribution from intensely cultivated floodplain regions (Galy et al., 2007; Garzanti et al., 2011). Considering this, the local sediment loss from the High Himalayas represents about half the observed gravity decrease, while in the Lesser Himalayas it is about 4 % (Table 4).

3.4.4 Impact within floodplain regions

To estimate the impact of sediment discharge on gravity data of groundwater depletion, we are interested in erosion within the Indo–Gangetic floodplain, where the strongest gravity decrease is observed. Generally, the estimation of the sediment impact in river lowlands and floodplains is more complicated due to sedimentary redistribution within the catchments. While some sediment might be eroded in regions of excessive agriculture (Galy et al., 2007; Garzanti et al., 2011), there might also be regions of sediment storage and river accretion. Wasson (2003) estimated the fraction of Ganges sediment discharge that was eroded from floodplain regions to be < 10 %. As an upper estimate, we assume this 10 % of Ganges sediment to be eroded directly within the floodplain section that yields the strongest GRACE gravity reduction (part of the Ganges catchment bound by 76 to 79° E and 28 to 30° N). For this area, the sediment loss would represent a mass loss of roughly $0.9\,\mathrm{kg\,m^{-2}\,yr^{-1}}$ and would explain at most 2 % of the observed TWS decrease in this region ($5.4\,\mathrm{cm\,yr^{-1}}$). Most likely, the floodplain sediment would be eroded more homogeneously from the catchment, reducing

the impact to less than 1 % of the observed gravity decrease. Thus, despite high sediment discharge by Indian rivers, the impact of sediment mass loss on TWS trends in the floodplains is comparatively small.

3.5 Impact of the Himalaya uplift on geodetic observations of trends in terrestrial water storage

Sediment discharge is not the only process that impacts TWS trends from satellite gravimetry. One other process significant in the Himalayan study area is mountain orogeny. The Indian and Eurasian continental plates collide at a speed of about $50\,\mathrm{mm\,yr^{-1}}$ (Larson et al., 1999). This causes an uplift of the Himalayan mountain range (Bisht et al., 2021) and consequentially a mass increase within this collision region. Similar to the sediment transport by rivers, such tectonic processes have so far been considered too small to be observed via satellite gravimetry (Mikhailov et al., 2004). However, like the signal of sediment transport, this gravity change becomes relevant when studying trends over long time periods.

While the tectonic impact on satellite gravimetry is not the focus of our study, it is relevant in order to contextualize and interpret our study as well as for potential future application of our study results. Since the Indian Plate moves below the Eurasian Plate, the tectonic uplift is present in the Himalayan mountain ranges and in the Tibetan Plateau but not in the Indian floodplains (Li et al., 2020). We derived an estimate of the associated mass increase based on published uplift data (Xu et al., 2000; Fu and Freymueller, 2012; Bisht et al., 2021). For the Ganges and Brahmaputra mountain ranges, we find mass increases of $(0.8 \pm 1.1) \times 10^{12}$ and $(1.1 \pm 1.2) \times 10^{12}\,\mathrm{kg\,yr^{-1}}$, respectively. Details can be found in the Supplement.

This mass increase caused by orogenic uplift in the Himalayan mountains is in the same order of magnitude as the mass reduction by the sediment transport in rivers. While both processes are present in the mountain ranges, uplift effects the full area and sediment erosion is the strongest along the river paths. However, at the current satellite resolution it is not possible to separate the two processes. Thus, the gravimetric impact of tectonic processes should be studied further and needs to be combined with the impact of sediment transport before attempting a correction of TWS trends from satellite gravimetry along tectonically active mountain ranges.

4 Conclusions

Our study shows the impact of sediment erosion on gravimetric estimates of TWS loss within the main river catchments on the Indian subcontinent. Sediment erosion within the combined Ganges, Brahmaputra, Meghna and Indus catchments yields an average mass loss of $(0.5 \pm 0.2)\,\mathrm{kg\,m^{-2}\,yr^{-1}}$, which potentially causes 4 % of the observed gravity decrease currently attributed to groundwater loss. Exclusion of the Indus catchment increases the sediment impact to approximately 5 %.

Comparison of the sediment mass loss for individual river catchments yields the highest impact for the Brahmaputra catchment. There, sediment mass loss is $(1.1 \pm 0.4)\,\mathrm{kg\,m^{-2}\,yr^{-1}}$, corresponding to almost 8 % of observed gravity decrease within this catchment. In the Ganges catchment, sediment transport represents 3.3 % of the gravity decrease, while for the Meghna and Indus catchments its 2.2 % and 1.3 %, respectively.

Mountain regions are especially prone to erosion. Thus, the impact of sediment mass loss on satellite gravimetry is especially important for mountain ranges. Over the whole Ganges and Brahmaputra mountain range, we find sediment mass loss of $(2.2 \pm 1.0)\,\mathrm{kg\,m^{-2}\,yr^{-1}}$ with average loss of $(3.4 \pm 1.8)\,\mathrm{kg\,m^{-2}\,yr^{-1}}$ in the Ganges mountains and $(1.7 \pm 0.7)\,\mathrm{kg\,m^{-2}\,yr^{-1}}$ in the Brahmaputra mountains. This represents 22 % and 10 % of the observed gravity decrease in the Ganges and Brahmaputra mountains, respectively. Inspection of previously stated erosion hotspots indicates that the sediment loss could potentially explain up to 77 % of the gravity decrease in selected mountain regions.

However, investigation of the gravity increase caused by mountain orogeny yields data in the same order of magnitude as the gravity decrease by sediment discharge. Both processes are present mainly in the catchment mountain fractions, and at the current satellite resolution it is not possible to separate the two processes. Thus, further studies of spatial distributions in sediment erosion and mountain orogeny are needed to better constrain their combined impact on satellite gravimetry over tectonically active areas.

In the river floodplains, where gravimetric measurements show the strongest decrease, the sediment impact is much smaller than over the mountains. The strongest gravity decrease is observed in north-west India with a reduction of up to 5.8 cm of EWH per year. In this area, we find the sediment impact to be at most 2 % with less than 1 % over the whole floodplain area.

Code and data availability. Post-processed TWS data were used from the COST-G Level-3 data product (https://doi.org/10.5880/COST-G.GRAVIS_01_L3_TWS, Boergens et al., 2020). Catchment areas are from the HydroBASINS data product (https://www.hydrosheds.org/, Lehner and Grill, 2013). Sediment data were compiled from various studies as stated in Table 3. Precipitation data are from the ERA5 reanalyses (https://doi.org/10.24381/cds.adbb2d47, Hersbach et al., 2023). Data displayed in the figures can be requested from the corresponding author. Data analysis was performed in Python, utilizing the SciPy package (Virtanen et al., 2020) for least-squares analysis and interpolation.

Supplement. The supplement related to this article is available online at: https://doi.org/10.5194/hess-28-1527-2024-supplement.

Author contributions. AK and TW developed the concept of the study. AK performed the analysis and led the writing of the paper. MW and JM contributed to the interpretation of geodetic data. TR helped interpret the sediment data. HB, JN and CL contributed to the general data interpretation. All authors discussed results and commented on the manuscript.

Competing interests. The contact author has declared that none of the authors has any competing interests.

Disclaimer. Publisher's note: Copernicus Publications remains neutral with regard to jurisdictional claims made in the text, published maps, institutional affiliations, or any other geographical representation in this paper. While Copernicus Publications makes every effort to include appropriate place names, the final responsibility lies with the authors.

Acknowledgements. We express our gratitude to Maxime Mouyen and an anonymous referee for their insightful and constructive feedback, which enhanced the quality of this paper.

Financial support. This study in these interdisciplinary realms of geodesy and climate research was enabled by funding from the Norddeutscher Wissenschaftspreis (North German Science Prize).

The article processing charges for this open-access publication were covered by the University of Bremen.

Review statement. This paper was edited by Laurent Pfister and reviewed by Maxime Mouyen and one anonymous referee.

References

Akter, J., Roelvink, D., and van der Wegen, M.: Process-based modeling deriving a long-term sediment budget for the Ganges-Brahmaputra-Meghna Delta, Bangladesh, Estuar. Coast. Shelf S., 260, 107509, https://doi.org/10.1016/j.ecss.2021.107509, 2021.

Bisht, H., Kotlia, B. S., Kumar, K., Dumka, R. K., Taloor, A. K., and Upadhyay, R.: GPS derived crustal velocity, tectonic deformation and strain in the Indian Himalayan arc, Quatern. Int., 575–576, 141–152, https://doi.org/10.1016/j.quaint.2020.04.028, sI: Remote Sensing and GIS Applications in Quaternary Sciences, 2021.

Boergens, E., Dobslaw, H., and Dill, R.: COST-G GravIS RL01 Continental Water Storage Anomalies. V. 0004, GFZ Data Services, https://doi.org/10.5880/COST-G.GRAVIS_01_L3_TWS, 2020.

Boergens, E., Dobslaw, H., and Dill, R.: COST-G GravIS RL01 Continental Water Storage Anomalies. V. 0005, GFZ Data Services [data set], https://doi.org/10.5880/COST-G.GRAVIS_01_L3_TWS, 2020.

Borrelli, P., Robinson, D. A., Fleischer, L. R., Lugato, E., Ballabio, C., Alewell, C., Meusburger, K., Modugno, S., Schütt, B., Ferro, V., Bagarello, V., Oost, K. V., Montanarella, L., and Panagos, P.: An assessment of the global impact of 21st century land use change on soil erosion, Nat. Commun., 8, 2013, https://doi.org/10.1038/s41467-017-02142-7, 2017.

Burbank, D. W., Bookhagen, B., Gabet, E. J., and Putkonen, J.: Modern climate and erosion in the Himalaya, C. R. Geosci., 344, 610–626, https://doi.org/10.1016/j.crte.2012.10.010, erosion–Alteration: from fundamental mechanisms to geodynamic consequences (Ebelmen's Symposium), 2012.

Cannon, F., Carvalho, L. M. V., Jones, C., and Bookhagen, B.: Multi-annual variations in winter westerly disturbance activity affecting the Himalaya, Clim. Dynam., 44, 441–455, https://doi.org/10.1007/s00382-014-2248-8, 2015.

Cazenave, A., Dominh, K., Guinehut, S., Berthier, E., Llovel, W., Ramillien, G., Ablain, M., and Larnicol, G.: Sea level budget over 2003–2008: A reevaluation from GRACE space gravimetry, satellite altimetry and Argo, Global Planet. Change, 65, 83–88, https://doi.org/10.1016/j.gloplacha.2008.10.004, 2009.

Coleman, J. M.: Brahmaputra river: Channel processes and sedimentation, Sediment. Geol., 3, 129–239, https://doi.org/10.1016/0037-0738(69)90010-4, brahmaputra river: Channel processes and sedimentation, 1969.

Curray, J. R.: Sediment volume and mass beneath the Bay of Bengal, Earth Planet. Sc. Lett., 125, 371–383, https://doi.org/10.1016/0012-821X(94)90227-5, 1994.

Dahle, C. and Murböck, M.: Post-processed GRACE/GRACE-FO Geopotential GSM Coefficients COST-G RL01 (Level-2B Product). V. 0002., GFZ Data Services., https://doi.org/10.5880/COST-G.GRAVIS_01_L2B, 2020.

Dahle, C., Murböck, M., Flechtner, F., Dobslaw, H., Michalak, G., Neumayer, K. H., Abrykosov, O., Reinhold, A., König, R., Sulzbach, R., and Förste, C.: The GFZ GRACE RL06 Monthly Gravity Field Time Series: Processing Details and Quality Assessment, Remote Sens.-Basel, 11, 2116, https://doi.org/10.3390/rs11182116, 2019.

Faisal, B. M. R. and Hayakawa, Y. S.: Geomorphological processes and their connectivity in hillslope, fluvial, and coastal areas in Bangladesh: A review, Progress in Earth and Planetary Science, 9, 41, https://doi.org/10.1186/s40645-022-00500-8, 2022.

FAO: AQUASTAT Core Database, Food and Agriculture Organization of the United Nations, https://tableau.apps.fao.org/views/ReviewDashboard-v1/country_dashboard?%3Aembed=y&%3AisGuestRedirectFromVizportal=y (last access: 17 November 2022), 2022.

Fu, Y. and Freymueller, J. T.: Seasonal and long-term vertical deformation in the Nepal Himalaya constrained by GPS and GRACE measurements, J. Geophys. Res.-Sol. Ea., 117, B03407, https://doi.org/10.1029/2011JB008925, 2012.

Galy, V., France-Lanord, C., Beyssac, O., Faure, P., Kudrass, H., and Palhol, F.: Efficient organic carbon burial in the Bengal fan sustained by the Himalayan erosional system, Nature, 450, 407–410, https://doi.org/10.1038/nature06273, 2007.

Garzanti, E., Andó, S., France-Lanord, C., Censi, P., Vignola, P., Galy, V., and Lupker, M.: Mineralogical and chemical variability of fluvial sediments 2. Suspended-load silt (Ganga–Brahmaputra, Bangladesh), Earth Planet. Sc. Lett., 302, 107–120, https://doi.org/10.1016/j.epsl.2010.11.043, 2011.

Giosan, L., Constantinescu, S., Clift, P. D., Tabrez, A. R., Danish, M., and Inam, A.: Recent morphodynamics of the Indus delta shore and shelf, Cont. Shelf Res., 26, 1668–1684, https://doi.org/10.1016/j.csr.2006.05.009, 2006.

GLCNMO: Global Land Cover by National Mapping Organizations: GLCNMO Version 3, Geospatial Information Authority of Japan, Chiba University and Collaborating Organizations, https://github.com/globalmaps/gm_lc_v3 (last access: 26 November 2022), 2017.

GRDC: Major River Basins of the World: "Major Rivers", 2nd, rev. ext. edn., Global Runoff Data Centre, Federal Institute of Hydrology (BfG), Koblenz, Germany, https://www.bafg.de/SharedDocs/ExterneLinks/GRDC/mrb_shp_zip.html;jsessionid=993792470F4B2723B3942ACFA8C09C66.live11313?nn=201762 (last access: 24 November 2022), 2020.

Hersbach, H., Bell, B., Berrisford, P., Biavati, G., Horányi, A., Muñoz Sabater, J., Nicolas, J., Peubey, C., Radu, R., Rozum, I., Schepers, D., Simmons, A., Soci, C., Dee, D., and Thépaut, J.-N.: ERA5 hourly data on single levels from 1940 to present, Copernicus Climate Change Service (C3S) Climate Data Store (CDS) [data set], https://doi.org/10.24381/cds.adbb2d47, 2023.

Holeman, J. N.: The Sediment Yield of Major Rivers of the World, Water Resour. Res., 4, 737–747, https://doi.org/10.1029/WR004i004p00737, 1968.

Islam, S.: Deltaic floodplains development and wetland ecosystems management in the Ganges–Brahmaputra–Meghna Rivers Delta in Bangladesh, Sustainable Water Resources Management, 2, 237–256, https://doi.org/10.1007/s40899-016-0047-6, 2016.

Jacob, T., Wahr, J., Pfeffer, W. T., and Swenson, S.: Recent contributions of glaciers and ice caps to sea level rise, Nature, 482, 514–518, https://doi.org/10.1038/nature10847, 2012.

Jarvis, A., Reuter, H., Nelson, A., and Guevara, E.: Hole-filled seamless SRTM data V4, International Centre for Tropical Agriculture (CIAT), https://srtm.csi.cgiar.org (last access: 24 November 2022), 2008.

Jeon, T., Seo, K.-W., Youm, K., Chen, J., and Wilson, C. R.: Global sea level change signatures observed by GRACE satellite gravimetry, Sci. Rep., 8, 13519, https://doi.org/10.1038/s41598-018-31972-8, 2018.

Kuehl, S. A., Allison, M. A., Goodbred, S. L., and Kudrass, H.: The Ganges–Brahmaputra Delta, in: River Deltas–Concepts, Models, and Examples, SEPM Society for Sedimentary Geology, https://doi.org/10.2110/pec.05.83.0413, 2005.

Larson, K. M., Bürgmann, R., Bilham, R., and Freymueller, J. T.: Kinematics of the India-Eurasia collision zone from GPS measurements, J. Geophys. Res.-Sol. Ea., 104, 1077–1093, https://doi.org/10.1029/1998JB900043, 1999.

Lehner, B. and Grill, G.: Global river hydrography and network routing: baseline data and new approaches to study the world's large river systems, Hydrol. Process., 27, 2171–2186, https://doi.org/10.1002/hyp.9740 2013 (data available at: https://www.hydrosheds.org/, last access: 6 October 2022)

Li, L., Murphy, M. A., and Gao, R.: Subduction of the Indian Plate and the Nature of the Crust Beneath Western Tibet: Insights From Seismic Imaging, J. Geophys. Res.-Sol. Ea., 125, e2020JB019684, https://doi.org/10.1029/2020JB019684, 2020.

Li, Z., Zhang, Z., Scanlon, B. R., Sun, A. Y., Pan, Y., Qiao, S., Wang, H., and Jia, Q.: Combining GRACE and satellite altimetry data to detect change in sediment load to the Bohai Sea, Sci. Total Environ., 818, 151677, https://doi.org/10.1016/j.scitotenv.2021.151677, 2022.

Luthcke, S. B., Sabaka, T., Loomis, B., Arendt, A., McCarthy, J., and Camp, J.: Antarctica, Greenland and Gulf of Alaska land-ice evolution from an iterated GRACE global mascon solution, J. Glaciol., 59, 613–631, https://doi.org/10.3189/2013JoG12J147, 2013.

Mahmud, M. I., Mia, A. J., Islam, M. A., Peas, M. H., Farazi, A. H., and Akhter, S. H.: Assessing bank dynamics of the Lower Meghna River in Bangladesh: an integrated GIS-DSAS approach, Arab. J. Geosci., 13, 602, https://doi.org/10.1007/s12517-020-05514-4, 2020.

Mikhailov, V., Tikhotsky, S., Diament, M., Panet, I., and Ballu, V.: Can tectonic processes be recovered from new gravity satellite data?, Earth Planet. Sc. Lett., 228, 281–297, https://doi.org/10.1016/j.epsl.2004.09.035, 2004.

Milliman, J. D. and Meade, R. H.: World-Wide Delivery of River Sediment to the Oceans, J. Geol., 91, 1–21, http://www.jstor.org/stable/30060512 (last access: 8 March 2024), 1983.

Mouyen, M., Longuevergne, L., Steer, P., Crave, A., Lemoine, J.-M., Save, H., and Robin, C.: Assessing modern river sediment discharge to the ocean using satellite gravimetry, Nat. Commun., 9, 3384, https://doi.org/10.1038/s41467-018-05921-y, 2018.

Panda, D. K. and Wahr, J.: Spatiotemporal evolution of water storage changes in India from the updated GRACE-derived gravity records, Water Resour. Res., 52, 135–149, https://doi.org/10.1002/2015WR017797, 2016.

Rahman, M., Dustegir, M., Karim, R., Haque, A., Nicholls, R. J., Darby, S. E., Nakagawa, H., Hossain, M., Dunn, F. E., and Akter, M.: Recent sediment flux to the Ganges-Brahmaputra-Meghna delta system, Sci. Total Environ., 643, 1054–1064, https://doi.org/10.1016/j.scitotenv.2018.06.147, 2018.

Rodell, M., Velicogna, I., and Famiglietti, J. S.: Satellite-based estimates of groundwater depletion in India, Nature, 460, 999–1002, https://doi.org/10.1038/nature08238, 2009.

Rodell, M., Famiglietti, J. S., Wiese, D. N., Reager, J. T., Beaudoing, H. K., Landerer, F. W., and Lo, M.-H.: Emerging trends in global freshwater availability, Nature, 557, 651–659, https://doi.org/10.1038/s41586-018-0123-1, 2018.

Schnitzer, S., Seitz, F., Eicker, A., Güntner, A., Wattenbach, M., and Menzel, A.: Estimation of soil loss by water erosion in the Chinese Loess Plateau using Universal Soil Loss Equation and GRACE, Geophys. J. Int., 193, 1283–1290, https://doi.org/10.1093/gji/ggt023, 2013.

Siebert, S., Burke, J., Faures, J. M., Frenken, K., Hoogeveen, J., Döll, P., and Portmann, F. T.: Groundwater use for irrigation – a global inventory, Hydrol. Earth Syst. Sci., 14, 1863–1880, https://doi.org/10.5194/hess-14-1863-2010, 2010.

Smith, G. S., Best, J. L., Bristow, C. S., and Petts, G. E.: Braided Rivers: process, deposits, ecology and management, https://www.wiley.com/en-us/Braided+Rivers:+Process,+Deposits,+Ecology+and+Management-p-9781444304374 (last access: 20 October 2022), 2009.

Subramanian, V. and Ramanathan, A. L.: Nature of Sediment Load in the Ganges-Brahmaputra River Systems in India, Springer Netherlands, Dordrecht, https://doi.org/10.1007/978-94-015-8719-8_8, 151–168, 1996.

Tiwari, V. M., Wahr, J., and Swenson, S.: Dwindling groundwater resources in northern India, from satellite gravity observations, Geophys. Res. Lett., 36, L18401, https://doi.org/10.1029/2009GL039401, 2009.

Virtanen, P., Gommers, R., Oliphant, T. E., Haberland, M., Reddy, T., Cournapeau, D., Burovski, E., Peterson, P., Weckesser, W., Bright, J., van der Walt, S. J., Brett, M., Wilson, J., Millman, K. J., Mayorov, N., Nelson, A. R. J., Jones, E., Kern, R., Larson, E., Carey, C. J., Polat, I., Feng, Y., Moore, E. W., VanderPlas, J., Laxalde, D., Perktold, J., Cimrman, R., Henriksen, I., Quintero, E. A., Harris, C. R., Archibald, A. M., Ribeiro, A. H., Pedregosa, F., and van Mulbregt, P.: SciPy 1.0: Fundamental Algorithms for Scientific Computing in Python, Nat. Methods, 17, 261–272, https://doi.org/10.1038/s41592-019-0686-2, 2020.

Wada, Y., van Beek, L. P. H., and Bierkens, M. F. P.: Nonsustainable groundwater sustaining irrigation: A global assessment, Water Resour. Res., 48, W00L06, https://doi.org/10.1029/2011WR010562, 2012.

Wasson, R. J.: A sediment budget for the Ganga–Brahmaputra catchment, Current Science, 84, 1041–1047, http://www.jstor.org/stable/24107666 (last access: 8 March 2024), 2003.

Wilson, C. A. and Goodbred, S. L.: Construction and Maintenance of the Ganges–Brahmaputra–Meghna Delta: Linking Process, Morphology, and Stratigraphy, Annu. Rev. Mar. Sci., 7, 67–88, https://doi.org/10.1146/annurev-marine-010213-135032, 2015.

Xie, H., Longuevergne, L., Ringler, C., and Scanlon, B.: Integrating groundwater irrigation into hydrological simulation of India: Case of improving model representation of anthropogenic water use impact using GRACE, Journal of Hydrology: Regional Studies, 29, 100681, https://doi.org/10.1016/j.ejrh.2020.100681, 2020.

Xu, C., Liu, J., Song, C., Jiang, W., and Shi, C.: GPS measurements of present-day uplift in the Southern Tibet, Earth Planet. Space, 52, 735–739, https://doi.org/10.1186/BF03352274, 2000.